RSC Advances

PAPER

Cite this: *RSC Adv.*, 2021, **11**, 27689

A process of leaching recovery for cobalt and lithium from spent lithium-ion batteries by citric acid and salicylic acid

Meiling Xu,[a] Shumei Kang,*[a] Feng Jiang,[b] Xinyong Yan,[a] Zhongbo Zhu,[a] Qingping Zhao,[a] Yingxue Teng[a] and Yu Wang[a]

There is great economic and environmental value in recovering valuable metal ions from spent lithium-ion batteries (LIBs). A novel method that employs organic acid recovery using citric acid and salicylic acid was used to enhance the leaching of metal ions from the cathode materials of spent LIBs. The effects of the acid concentration, reducing agent content, solid to liquid (S : L) ratio, temperature, and leaching time were systematically analyzed and the optimal acid leaching process condition was determined through the results. The kinetics of the leaching process with different temperatures was analyzed to explore and verify the relationship between the leaching mechanism and temperature. The results of TG/DSC analysis showed that the optimum calcination temperature was 500 °C for 1 h and 600 °C for 3 h. The XRD and micromorphology analysis results showed that cathode material powders without impurities were obtained after pretreatment. The experimental results demonstrated that the optimal leaching efficiencies of the metals ions were 99.5% Co and 97% Li and the optimal corresponding condition was 1.5 M citric acid, 0.2 M salicylic acid, a 15 g L^{-1} S : L ratio, 6 vol% H_2O_2, 90 °C, and 90 min. Afterward, the infrared tests and SEM morphologies results indicated that only salicylic acid was present in the residue after filtration because of the microsolubility of the salicylic acid. Finally, it was obvious that the temperature had a great influence on the leaching process as observed through the kinetics and thermodynamics analyses, while the E_a values for Co and Li were obtained as 37.96 kJ mol^{-1} and 25.82 kJ mol^{-1} through the kinetics model. The whole process was found to be efficient and reasonable for recovering valuable metals from the industrial electrodes of spent LIBs.

Received 28th June 2021
Accepted 2nd August 2021

DOI: 10.1039/d1ra04979h

rsc.li/rsc-advances

1 Introduction

Lithium-ion batteries (LIBs) have been considered to be one of the most popular types of rechargeable batteries in portable electronic devices since the 1990s.[1,2] They are usually composed of valuable metals (Co, Li, Ni, Mn)/metal oxides, organic chemicals, metal casings, and plastics, and their proportions vary depending on the battery manufacturer and type.[3,4] They have been widely used in mobile electronic devices, such as mobile phones, laptops, computers, and also universally applied in military, aerospace, navigation, electric vehicles, and medical equipment. In recent years, the LIB industry has witnessed explosive growth. At present, China has become the main country in the production, consumption, and exporting of LIBs.[5,6] Environmental pollution and the global energy crisis have driven significant progress in new sources of energy for vehicles and the consequent boom in the production and use of LIBs.[7–10] There is no doubt that this boom will lead to a large number of spent LIBs.[11–13] Therefore, research into an environmentally friendly and efficient recycling process for spent LIBs is urgently needed.

Currently, the research methods for recovering valuable metals from spent LIBs are mainly pyrometallurgy, hydrometallurgy, and biohydrometallurgy.[14] Due to the high energy consumption and harmful gas produced in pyrometallurgy, it has not been widely used in the research work.[15,16] As a new technology for the treatment of recycling spent materials, biohydrometallurgy has attracted wide interest and holds great promise. However, biohydrometallurgy is inefficient in the treatment of spent LIBs with a high metal content.[17] Therefore, the hydrometallurgical process with high efficiency and good environmental friendliness is a good alternative for recovering valuable metals from spent LIBs. At this stage, the leaching system of spent LIBs mainly involves "inorganic acid + reducing agent" system or "organic acid + reducing agent" systems.[18] The leaching system involving an "inorganic acid + reducing agent" has been applied in the field of factory production. The "inorganic acid + reducing agent" system is widely used, but harmful gases will be produced in the process of acid leaching, and the

[a]School of Materials and Metallurgy, University of Science and Technology Liaoning, Anshan, 114051, China. E-mail: kangshumei_911@163.com
[b]Department of Materials Science and Engineering, Southern University of Science and Technology, Shenzhen, 518055, China

waste acid after leaching is difficult to treat, which will pose potential harm to the environment.[19,20] At this time, the leaching system "organic acid + reducing agent" emerges as required in modern times. Therefore, research using organic acid systems for efficient recovery spent LIBs has become a new research focus.[21,22] Table 1 summarizes the different leaching systems for recovering metals from spent lithium cobalt oxide (LCO) batteries in recent years.

Based on the current research, a new mixed organic acid of citric acid and salicylic acid is proposed to recover valuable metal ions from spent LIBs, with H_2O_2 used as the reducing agent in the leaching process. Salicylic acid is usually used as the main ingredient of medicines and cosmetics. Compared with other organic acids, such as ascorbic acid and tartaric acid, salicylic acid is environmentally friendly and harmless. It is an organic acid with excellent performance that has not been used much yet. The addition of salicylic acid can improve the complexation ability between acid and ions, and a small amount of salicylic acid can reduce the excessive use of citric acid and improve the leaching efficiencies of Co and Li ions. In this work, the spent cathode material was pretreated to remove impurities, and TG/DSC analysis was used to determine the optimal pretreatment temperature. The phase composition and morphology of LIBs before and after leaching were investigated, and the kinetics and thermodynamics of the organic acid leaching process were analyzed, together with the optimization of various operating parameters. The purpose of this work was to improve the leaching efficiencies of Co and Li using green organic acids, and then to provide new ideas for the green recovery of spent LIBs in the future.

2 Experimental

2.1 Sample preparation and pretreatment process

Spent LIBs were collected from the Chinese market and first discharged in 10 wt% NaCl (Macklin, AR, 99.5%) solution for 24 h, and then the spent LIBs could be dismantled when the voltage measured by the voltmeter was less than 2 V. The lug and outer casing of the LIBs were removed with pliers, and then the anode electrode was carefully separated. The other internal structures of the LIBs, including the anode electrode, plastic and steel cases, and outer casing were recycled, respectively. Thermal pretreatment was necessary to eliminate the carbon and PVDF in the cathode materials. To determine the optimal temperature of thermal pretreatment, the cathode materials from the spent LIBs were analyzed by TG/DSC analysis (STA449 F3, Netzsch, Selb, Germany) in a N_2 atmosphere at a flow rate of 60 mL min^{-1}. About 4.0 mg sample was used for the TG/DSC analysis and was heated from 50 °C to 800 °C at a heating rate of 10 K min^{-1}. The powders were characterized by X-ray diffraction (XRD, LabX XRD-6000, Japan Shimadzu Co., Ltd., Tokyo, Japan) with Cu Kα radiation (1.5418 Å) at a voltage of 40 kV and 150 mA, and the data were collected in the 2θ range of 5–90° at a speed of 5° min^{-1}. The morphology of the cathode material was analyzed by scanning electron microscopy (SEM, JSM-6390A, Joint-stock Company, Beijing, China) under different magnifications at a 10 kV accelerating voltage, while the element type and content analysis were tested by energy dispersive spectrometer (EDS, JSM-6390A, Joint-stock Company, Beijing, China). Subsequently, the cathode material powders were ground in a mortar for 1 h to obtain smaller and higher specific surface area particles. This step was conducive to the subsequent improvement of dissolution rate and leaching efficiency. All the chemical reagents, including citric acid ($C_6H_8O_7$, Aladdin, AR, ≥99.5%) and salicylic acid ($C_7H_6O_3$, Aladdin, AR, 99.5%), used in this research were analytical grade and all the solutions were prepared or diluted by deionized water.

2.2 Experimental procedure for the leaching process

All the leaching experiments were carried out in a 250 mL three-necked round-bottomed flask equipped with a reflux condenser to avoid loss of water by evaporation and the three-necked round-bottomed reactor was placed in a water bath with a temperature controller and magnetic stirring. Above all, the cathode material powders were weighed on the basis of the solid to liquid (S : L) ratio (15–35 g L^{-1}), and then added to the mixed solution containing different concentrations of citric acid (0.5–2.5 M) and salicylic acid (0–0.3 M). Ultimately, H_2O_2 (1–6 vol%, Sinopharm Group, 30% H_2O_2, AR, 99.5%) was added to the acid solution as a reducing agent and the constant volume was 100 mL. During the leaching reaction, the ranges for the temperature and time were 30–90 °C and 15–120 min.

Table 1 Summary of the leaching systems for metals recovery from spent LCO batteries

Spent materials	Leaching reagents	Reaction conditions			Leaching efficiency (%)	Ref.
		Temp. (°C)	S/L ratio (g L^{-1})	Time (min)		
LCO	2 M H_2SO_4 + 5 vol% H_2O_2	75	100	30	Li = 94, Co = 93	23
	2 M H_2SO_4 + 8 vol% H_2O_2	70	20	60	Li = 99, Co = 99	24
	2 M H_2SO_4 + 5 vol% H_2O_2	80	50	60	Li = 99, Co = 99	25
	1 M H_2SO_4 +0.075 M $NaHSO_3$	95	20	240	Li = 97, Co = 92	26
	0.23 M $H_2C_2O_4$ + 3.6 vol% H_2O_2	100	15	180	Li = 91, Co = 97	27
	2 M citric acid + 0.6 g g^{-1} H_2O_2	90	15	30	Li = 100, Co = 91	28
	0.1 M citric acid + 0.02 M ascorbic acid	80	10	360	Li = 100, Co = 80	29
	57.8 vol% lemon juice + 8.07 vol% H_2O_2	60	9.8	45	Li = 100, Co = 96	30
	2 M L-tartaric acid + 4 vol% H_2O_2	70	17	30	Li = 99, Co = 96	31
	1.5 M succinic acid + 4 vol% H_2O_2	70	15	40	Li = 96, Co = 99.5	32

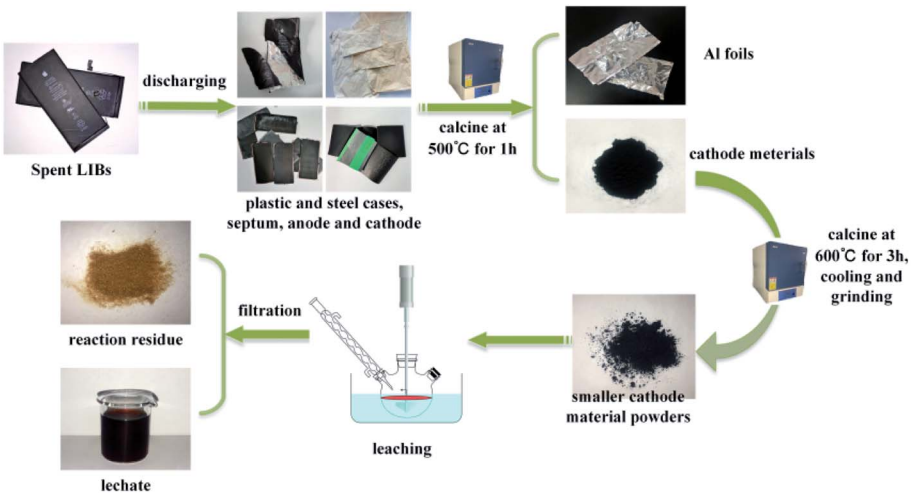

Fig. 1 Flowsheet of the procedure applied for metal recovery.

After leaching, the mixture (leachate and reaction residue) was filtered immediately. Meanwhile, the concentrations of Co and Li ions in the leachate obtained after leaching were determined by inductively coupled plasma optical emission spectrometry (ICP-OES, PDQ9000, Analytik Jena AG, Jena, Germany) to calculate the leaching efficiencies of Co and Li, while the contents of the functional groups of the substances in the leachate were qualitatively analyzed by infrared spectrometry (Cary 630FTIR, Agilent Technologies Inc., California, U.S). The effects of various factors on the leaching process were studied and determined. A flowsheet of the procedure applied for metal recovery in this research is illustrated in Fig. 1. The calculation formula for the leaching efficiency is represented as follows (eqn (1)):[33]

$$X = \frac{n \times C \times V_0}{m_0 \times \mathrm{wt}\%} \times 100\% \quad (1)$$

where X (%) is the leaching efficiency, n, C (g L^{-1}), and V_0 (L) are the dilution time, concentration of metal ions, and the volume of leaching liquid, respectively, while m_0 (g) and wt% are the mass and mass fraction of the metals in the cathode materials.

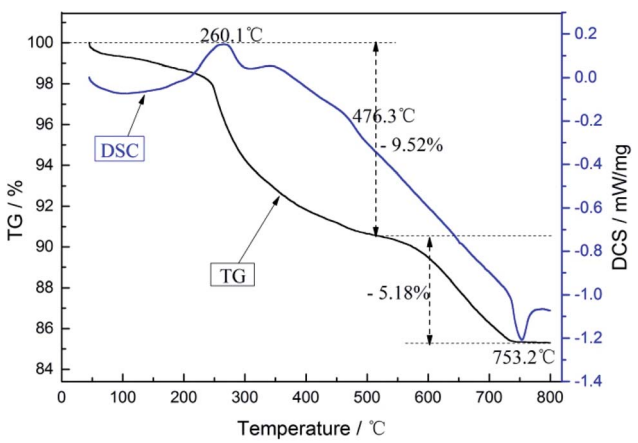

Fig. 2 TG/DSC curves of the cathode materials from the spent LIBs.

3 Results and discussion

3.1 Characteristics of the pretreatment cathode materials

Fig. 2 shows the TG/DSC curves of the cathode materials from the spent LIBs. From the TG curve, the first weight-loss region between 100 °C and 250 °C arose from the loss of ester compounds in the cathode materials, while the region between 250 °C and 550 °C corresponded to the pyrolysis of the organic binder and carbonaceous decomposition. When the temperature exceeded 600 °C, the loss of lithium appeared from $LiCoO_2$.[34] For the DSC curve, there two exothermic peaks could be seen at 260.1 °C and 476.3 °C, and one endothermic peak at 753.2 °C. These indicated that the exothermic peak at 260.1 °C was from the decomposition of the binder PVDF, while the exothermic peak at 476.3 °C indicated the oxidation decomposition of carbon, and the endothermic peak at 753.2 °C was from the endothermic reaction of the aluminum foil melting. Therefore, a two-step calcination method could be adopted. First, the cathode materials were heated to 500 °C at a rate of 5 °C min^{-1} and calcined for 1 h to make the cathode powders fall off the aluminum foil. Then, the shed powders were heated to 600 °C with the same heating rate and calcined for 3 h to remove any residual carbon. After calcination, the cathode powders were allowed to stand and cool down naturally to room temperature. Finally, the calcined cathode powders were immersed in 3 M NaOH solution for 2 h to remove the small amount of Al in the powders.

Fig. 3 shows the XRD patterns of the cathode powder before and after heat treatment, commercial $LiCoO_2$, cathode material from spent LIBs, and the standard JCPDS card for $LiCoO_2$. The XRD patterns displayed the most expected peaks for $LiCoO_2$. Fig. 3(a) demonstrated that peaks appeared for the crystal planes (003), (101), (104), (107), (018), (110), (113), and (024) of $LiCoO_2$. From the XRD results in Fig. 3(d), the cathode composition of the spent LIBs was mainly composed of $LiCoO_2$, C, PVDF, and $Al(OH)_3$. At 2θ angles of 37.38°, 39.06°, 66.32°, 79.32°, and 84.18°, $LiCoO_2$ peaks with the corresponding crystal planes (101), (012), (110), (116), and (024) appeared, respectively. The C peak appeared at a 2θ angle of 26.8° and the

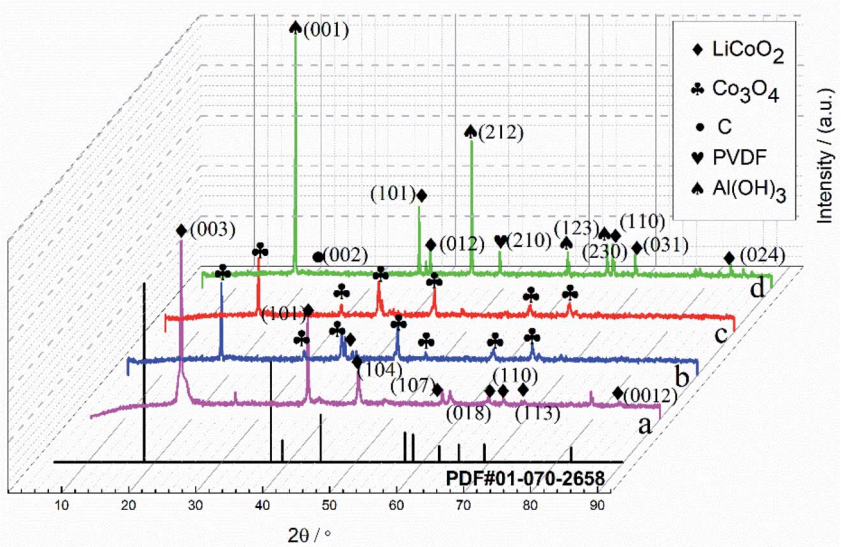

Fig. 3 XRD patterns of the powders: (a) commercial $LiCoO_2$; (b) cathode powders after calcination at 500 °C; (c) cathode powders after calcination at 600 °C; (d) cathode material from spent LIBs and the standard JCPDS card for $LiCoO_2$.

corresponding crystal plane of (002). The PVDF peak appeared at a 2θ angle of 49.42°, and the corresponding crystal plane of (210). $Al(OH)_3$ peaks with the corresponding crystal planes (001), (212), (123), (230), and (031) appeared at 2θ angles of 18.5°, 45.22°, 57.48°, 59.76°, and 65.6°, respectively. Among these, PVDF was the main component of the binder in the cathode material. The C element may come from the conductive spent anode layer.[35] The heat pretreatment reaction for PVDF decomposition and C oxidation decomposition are shown in eqn (2) and (3).[36]

$$[CH_2CF_2]_n^{2-} = 2nC + 2nHF + Q \quad (2)$$

$$C + O_2 = CO_2 + Q \quad (3)$$

Al in the cathode material can be oxidized and it is easy to produce $Al(OH)_3$ in humid air. The existence of these substances explains that there were many impurities in the unheated cathode materials. After heat pretreatment, as seen in Fig. 3(b) and (c), the XRD results indicated that both $LiCoO_2$ and Co_3O_4 peaks existed in the powders produced by calcination. In this experiment, when the calcination temperature was 500 °C, the cathode material powders will fall off and the aluminum foil will not be damaged; however the calcination was not uniform.

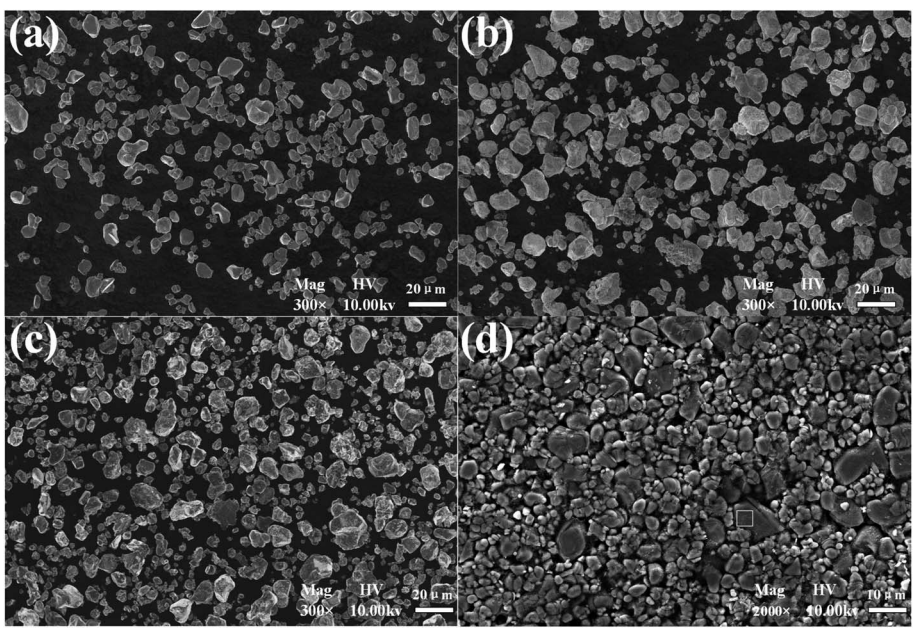

Fig. 4 SEM morphologies of powders: (a) commercial $LiCoO_2$; (b) cathode powders after calcination at 500 °C; (c) cathode powders after calcination at 600 °C; (d) cathode material from spent LIBs.

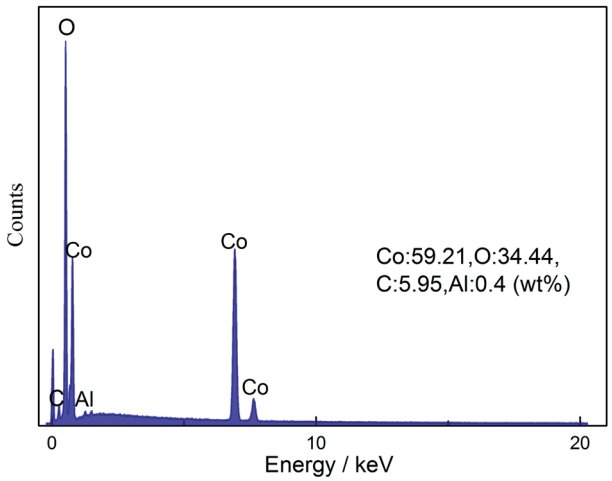

Fig. 5 EDS results of the cathode material from spent LIBs.

Therefore, when continuing to calcine at 600 °C for 3 h (Fig. 3(c)), $LiCoO_2$ and Co_3O_4 uniform powders were formed.

Fig. 4 presents the morphologies of the cathode material before and after heat pretreatment. Compared with commercial $LiCoO_2$, it is obvious that the shape of the cathode material from the spent LIBs (Fig. 4(d)) was irregular. The EDS results in Fig. 5 show that there was bare aluminum on the surface of the spent LIBs, which is consistent with the peak of $Al(OH)_3$ in Fig. 3(d). In addition, the surface of the cathode material from the spent LIBs was covered with block binder. After calcination at 500 °C, it can be clearly seen from Fig. 4(c) that the cathode materials were dispersed into smaller powders with the same size as commercial $LiCoO_2$. After calcination at 600 °C, the powders were finer and more uniform. Besides, the XRD results in Fig. 3 show that the phase structure for the cathode material was not changed.

3.2 Leaching process of Co and Li

3.2.1 Analysis of the leaching reaction mechanism. As a typical environmentally friendly and low-cost leaching agent, both citric acid ($C_6H_8O_7$) and salicylic acid ($C_7H_6O_3$) have the characteristics of organic acids, including pollution-free and recyclability. They are considered as efficient leaching agents for recovering valuable metals in spent LIBs. There are three carboxyl groups in the $C_6H_8O_7$ molecule. Theoretically, 1 M citric acid is dissociated into 3 M H^+ and salicylic acid has two steps of dissociation in solution. Because salicylic acid has intramolecular hydrogen bonds, which cause the second step of dissociation of salicylic acid being difficult to achieve. Therefore, the appearance of salicylic acid acidity is mainly the first step of dissociation. The acid ionization equations for citric acid[37] and salicylic acid can be given as follows:

$$H_3Cit = H_2Cit^- + H^+ \quad K_{a1} = 7.4 \times 10^{-4} \tag{4}$$

$$H_2Cit^- = HCit^{2-} + H^+ \quad K_{a2} = 1.7 \times 10^{-5} \tag{5}$$

$$HCit^{2-} = Cit^{3-} + H^+ \quad K_{a3} = 4.0 \times 10^{-7} \tag{6}$$

$$HO\text{–}PH\text{–}COOH = HO\text{–}PH\text{–}COO^- + H^+ \quad K_{a1} = 1.3 \times 10^{-3} \tag{7}$$

$$HO\text{–}PH\text{–}COO^- = O^-\text{–}PH\text{–}COO^- + H^+ \quad K_{a2} = 1.1 \times 10^{-13} \tag{8}$$

From eqn (7) and (8), the second step ionization of salicylic acid is far less energetic than the first step ionization, therefore, only the first step ionization of salicylic acid was considered in this experiment. During the leaching reaction, two kinds of leaching acids react with $LiCoO_2$, respectively. The leaching reaction of $LiCoO_2$ with citric acid in the presence of H_2O_2 can be divided into the following three steps:[30]

$$6H_3Cit(aq) + 2LiCoO_2(s) + H_2O_2(aq) \rightarrow 2Li^+(aq) + 6H_2Cit^-(aq) + 2Co^{2+}(aq) + 4H_2O + O_2(g) \tag{9}$$

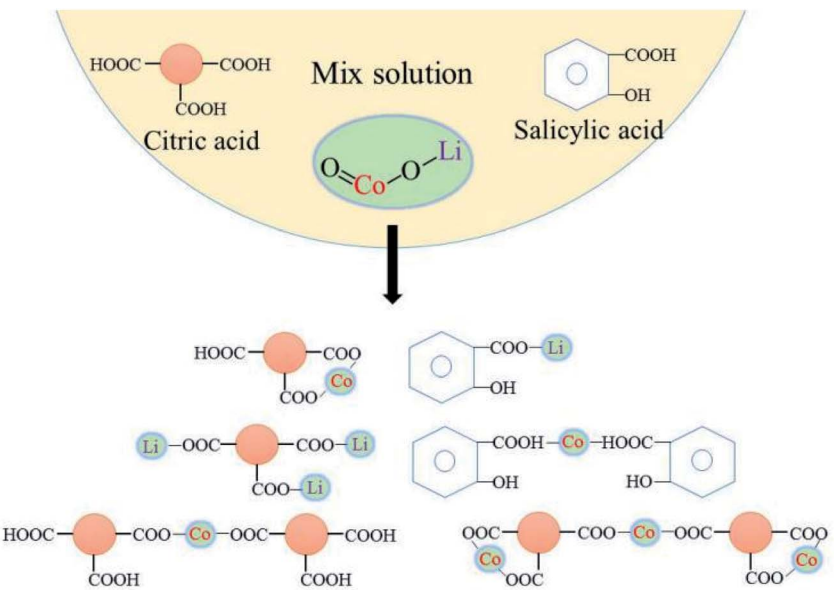

Fig. 6 Possible reaction products in the leaching environment.

$$6H_2Cit^-(aq) + 2LiCoO_2(s) + H_2O_2(aq) \rightarrow 2Li^+(aq) + 6HCit^{2-}(aq) + 2Co^{2+}(aq) + 4H_2O + O_2(g) \quad (10)$$

$$6HCit^{2-}(aq) + 2LiCoO_2(s) + H_2O_2(aq) \rightarrow 2Li^+(aq) + 6Cit^{3-}(aq) + 2Co^{2+}(aq) + 4H_2O + O_2(g) \quad (11)$$

In addition, 1 M salicylic acid released 1 M H^+. The leaching reaction of $LiCoO_2$ with salicylic acid in the presence of H_2O_2 is as follows (eqn (12)):

$$6HC_7H_5O_3(aq) + 2LiCoO_2(s) + H_2O_2(aq) \rightarrow 2Li^+(aq) + C_7H_5O_3^-(aq) + 2Co^{2+}(aq) + 4H_2O + O_2(g) \quad (12)$$

From eqn (9) to (12), it can be predicted that the addition of a reducing agent can promote the forward reaction. Here, eqn (9) and (12) are the main leaching reactions.[38] In the absence of a reductant, the oxygen in $LiCoO_2$ is partially oxidized to O_2, resulting in the low leaching efficiency of Co ions.[39] While under the action of a reductant, the high-cost transition metal Co(III) is easy to be reduced to the low-cost form Co(II), thus promoting the $LiCoO_2$ leaching. The possible reaction products of ions in the leaching environment are shown in Fig. 6. From Fig. 6, Co and Li ions are complexed and stabilized in solution, which makes the Co and Li elements from a solid phase to liquid phase. When the obtained cobalt complex, such as $Co(H_2Cit)_2$, $Co_3(Cit)_2$, and $Co(C_7H_5O_3)_2$, in solution reached the limit of solubility saturation, the activity product ($K_{sp} = \alpha_{Co} + \alpha_a$) usually remained constant. Excessive citric acid and salicylic acid could increase the solubility of H_2Cit^- and $C_7H_5O_3^-$ and decrease the solubility of Co ions. Therefore, it is expected that the separation of Co and Li can be selectively separated and recovered in a single step.[33] Moreover, the concentration of citric acid and salicylic acid will be critical for the leaching process.

3.2.2 Effect of acid concentration on the leaching efficiency. Fig. 7 shows the effect of different factors on the leaching efficiencies of Co and Li. Fig. 7(a) and (b) display the leaching efficiency results with different concentrations of citric acid and salicylic acid. The concentration of citric acid varied from 0.5 M to 2.5 M and that of salicylic acid varied from 0 to 0.3 M, while the S : L ratio was 20 g L^{-1}, the temperature was 70 °C, 4.5 vol% H_2O_2 was used, and the leaching time was 90 min. It could be observed that the concentration of citric acid had a greater influence on the leaching of Co and Li than that of salicylic acid. These results showed that the leaching efficiencies of Co and Li increased when the concentration of citric acid increased from 0.5 M to 2.5 M. When the concentration of citric acid was 1.5 M, the leaching efficiencies of Co and Li were 79.2% and 87.5%, respectively. In Fig. 7 (b), while the concentration of salicylic acid increased from 0 to 0.3 M, the leaching efficiency of Li did not change significantly but the leaching efficiency of Co increased significantly. The experimental results proved that the leaching efficiencies of Co and Li were 85.9% and 88.2% when the concentration of citric acid was 1.5 M and that of salicylic acid was 0.2 M. The results in Fig. 7(b) also indicated that a small amount of salicylic acid could improve the leaching efficiencies of Co and Li. In order to achieve the best leaching performance of $LiCoO_2$ in the whole leaching process, 1.5 M citric acid and 0.2 M salicylic acid were selected for the subsequent leaching experiments.

3.2.3 Effect of the S : L ratio on the leaching. Under the conditions of 70 °C, 1.5 M citric acid, 0.2 M salicylic acid, a leaching time of 90 min, and 4.5 vol% H_2O_2, the effect of the S : L ratio on the leaching efficiencies of Co and Li was studied. Fig. 7(c) shows that the leaching efficiencies of Co and Li increased with the decrease in S : L ratio. When the S : L ratio was 30 g L^{-1}, the leaching efficiencies of Co and Li were not very high. At 15 g L^{-1}, 93% Co and 90.9% Li could be leached. Therefore, the S : L ratio of 15 g L^{-1} was suitable for leaching the spent LIBs and 15 g L^{-1} was determined to be the optimum S : L ratio for leaching Co and Li from spent LIBs.

3.2.4 Effect of the reducing agent concentration on the leaching. The effect of the H_2O_2 concentration on the leaching results is shown in Fig. 7(d). During the leaching process, the temperature was kept at 70 °C, the S : L ratio was 15 g L^{-1}, citric acid concentration was 1.5 M, salicylic acid concentration was 0.2 M, and the leaching time was 90 min. The results showed that the leaching efficiencies of Co and Li increased significantly with the increase in H_2O_2 concentration. When the concentration of H_2O_2 increased to 6.0 vol%, the leaching efficiencies of Co and Li increased to 90.2% and 89.1%, respectively. In addition, Li was more soluble than Co in the presence of citric acid.[40] The experimental results showed that when too much H_2O_2 was added into the leaching solution, excessive boiling occurred in the leaching process, which affected the experimental results.

3.2.5 Effects of temperature and leaching time on the leaching. In this part, the effects of temperature and time on the leaching efficiency were studied. During the leaching process, the S : L ratio was kept at 15 g L^{-1} and the concentration of H_2O_2 was 6 vol%. The temperature was kept at 70 °C when studying the effect of the leaching time on the Co and Li-ions-leaching efficiency, and the leaching time was 90 min when studying the effect of temperature on the Co- and Li-ions-leaching efficiency. The experimental results are shown in Fig. 7 (e) and (f), and indicated that only 66.7% Co and 50.1% Li could be leached at the low temperature of 30 °C. These results showed that a low temperature is not conducive to the leaching of Co and Li from citric acid and salicylic acid. With the increase of temperature, the leaching efficiency of metals increased significantly, which indicated that temperature is an important factor affecting the metal-leaching efficiency. When the temperature rose to 50 °C, the leaching efficiencies of Co and Li exceeded 80.6% and 72.1%. At 70 °C, the leaching efficiencies of Co and Li reached 90%, which means they basically reached the leaching standard. At 90 °C, the leaching efficiency of Co was 99.5% and Li was 97.2%. At the same time, Fig. 7(e) shows that increasing the leaching time was beneficial for metal leaching. When the reaction time was less than 60 min, the leaching efficiencies of Co and Li increased significantly with the increase in reaction time. After 90 min, the leaching efficiencies of Co and Li did not increase significantly, indicating that the leaching reaction was nearly saturated. Based on the above conclusions, increasing the temperature significantly improved the metal-leaching efficiency, which was due to the dissociation

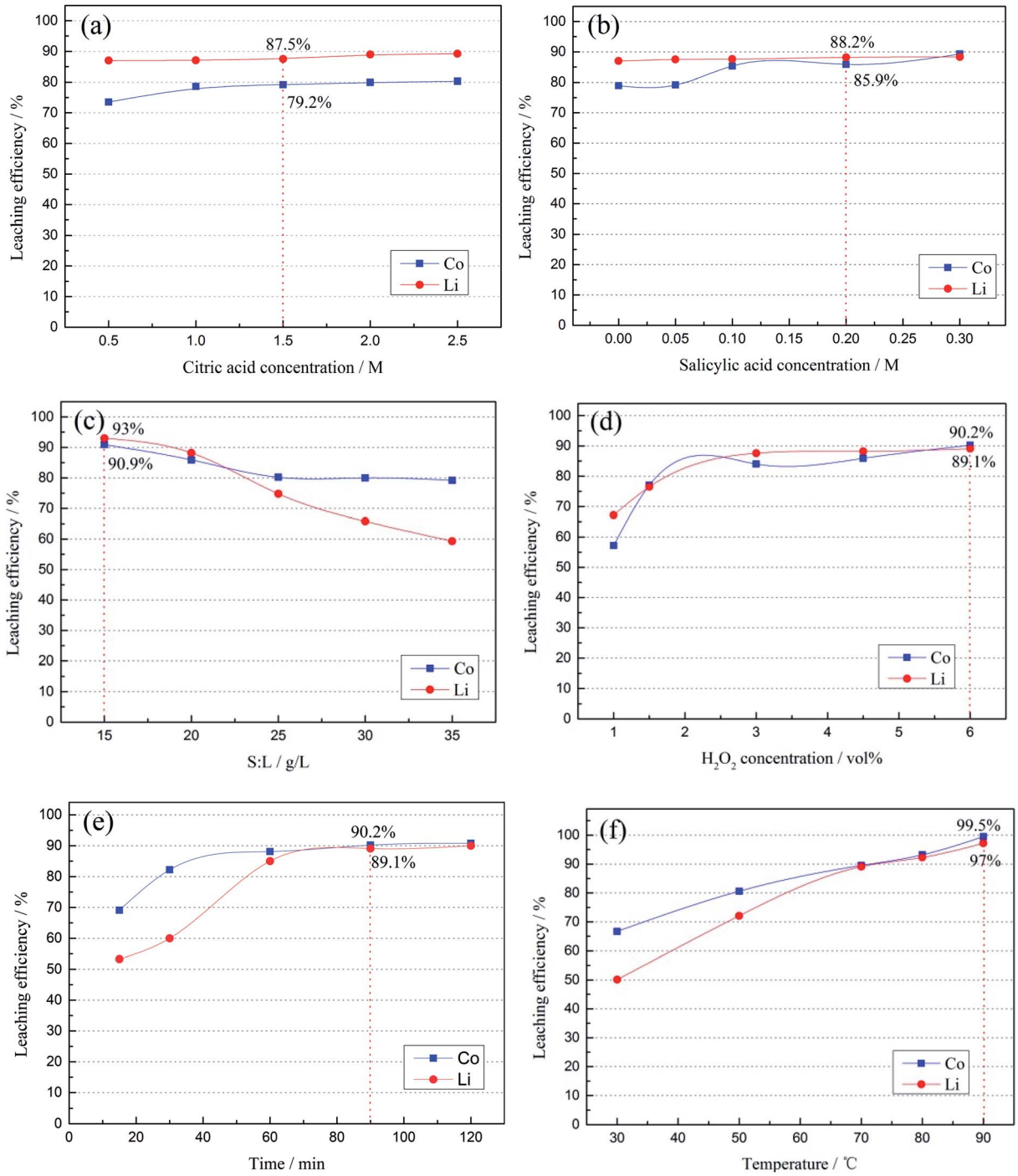

Fig. 7 Effect of different factors on the leaching efficiency: (a) citric acid concentration; (b) salicylic acid concentration; (c) S : L ratio; (d) H_2O_2 concentration; (e) time; (f) temperature.

processes of citric acid and salicylic acid being endothermic. With the increase in temperature, there were more H^+ in the solution. Therefore, the higher the leaching efficiencies of Co and Li, the faster the leaching effect of $LiCoO_2$. The next step of the reaction kinetics analysis further explains this point.

3.2.6 Characterization before and after leaching. According to the above leaching process, the optimum leaching conditions were: 1.5 M citric acid, 0.2 M salicylic acid, 4.5 vol% H_2O_2, S : L ratio of 15 g L^{-1}, leaching time of 90 min, and temperature of 70 °C. Under the optimum conditions, the characterization of the leachate and reaction residue was performed by infrared spectra analysis, and the results are shown in Fig. 8(a). From the analytical results of the infrared spectra for the leachate and reaction residue, significant changes in the stretching vibration and bending vibration could be detected for both the leachate and reaction residue after leaching. For the leachate, the

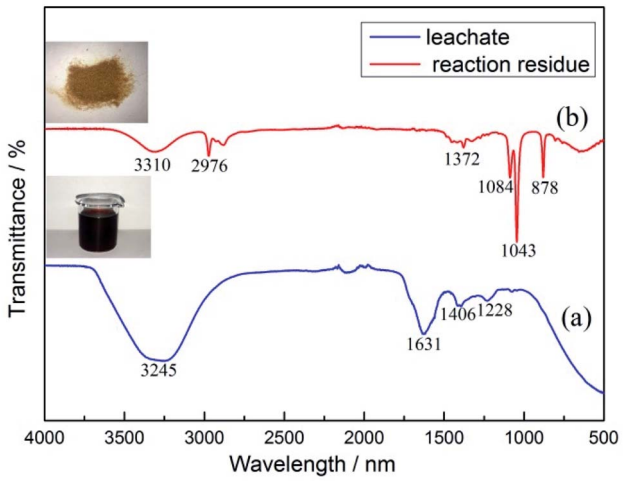

Fig. 8 Infrared spectra results of: (a) leachate; (b) reaction residue after leaching.

characteristic peaks after leaching at 3245, 1631, 1460, and 1228 indicated the changes in the unsaturated C–H stretch (alkenes, alkynes, aromatic compounds), unsaturated C–C stretch (aromatic compounds), C–H bending of alkanes, and C–O stretch of carboxylic acids and phenols, respectively. It was found that salicylic acid contained aromatic compounds, phenols, and carboxyl groups, and citric acid contained alkyl and carboxyl groups in the leaching solution. After filtration, the infrared spectra results of the reaction residue were obtained and are shown in Fig. 8(b). Completely different absorption peaks could be seen in the infrared spectra of the reaction residue. From the results, the characteristic peaks at 3310, 2976, 1372, 1086, and 878 represented the unsaturated C–H stretch (alkenes, alkynes, aromatic compounds), saturated C–H stretch (alkyl), C–H bending (alkanes), C–O stretch (phenols), and C–H bending of the olefins (aromatic compounds). The infrared spectra results indicated that citric acid and salicylic acid may have been present in the reaction residue after filtration. The solubility of salicylic acid was 0.22 g/100 g water at room temperature and 66 g/100 g in hot water, which is a slightly soluble substance. Therefore, salicylic acid must exist in the reaction residue at room temperature. Fig. 9 shows the SEM morphology of the reaction residue after leaching at 1000 and 100 magnification times. It can be seen that the reaction residue was a cuboid solid with a uniform distribution, as seen from the 100 times SEM image. After magnification to 1000 times, it could be more clearly seen that the leaching residue was rectangular. Combining the EDS results and all the peaks from the XRD results of the reaction residue in Fig. 9, it is obvious that there was only salicylic acid present in the reaction residue.

3.3 Reaction kinetics and thermodynamic parameters

To explore and verify the relationship between the leaching mechanism and leaching parameters, the kinetics of the leaching process at different temperatures was analyzed. The leaching reaction accorded with the shrinking core model, so the leaching process could be divided into the following steps:[41] (1) the leaching agent of citric acid and salicylic acid molecules diffuse through the solid–liquid interface; (2) these acid molecules diffuse to the surface of the unreacted core through the solid–liquid interface and are adsorbed by unreacted solids; (3) the adsorbed acid molecules react with unreacted solids and release products; (4) the reaction product falls off and reaches the solid–liquid interface through the reaction product layer; (5) the reaction product continues to diffuse into the fluid.

The leaching process of valuable metals from spent LIB cathodes is actually a solid–liquid–gas heterogeneous process, which can be described by the leaching kinetics in eqn (13):[42]

$$\frac{X}{3k_M}+\frac{R_0}{6D_e}\left[1-3(1-X)^{\frac{2}{3}}+2(1-X)\right]+\frac{1}{k_{rea}}\left[1-(1-X)^{\frac{1}{3}}\right]=\frac{MC_0}{x\rho R_0}\times t \quad (13)$$

where k_M is the mass-transfer coefficient in the liquid boundary layer, X is the reaction fraction (leaching efficiency), R_0 is the particle radius, D_e is the mass-transfer coefficient in the reaction product layer, k_{rea} is the reaction rate constant, M is the molar weight of cathode material, t is the leaching time, and C_0 is the acid concentration when t is 0, ρ is the density of cathode material, and x is the electron-transfer number in the reaction process.

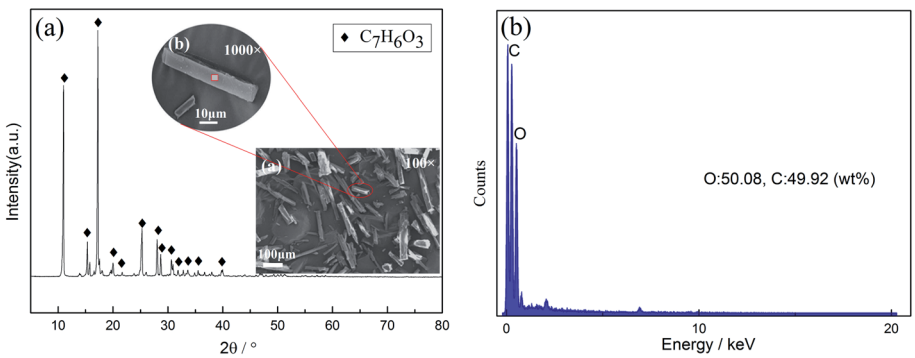

Fig. 9 (a) XRD patterns, SEM morphologies; (b) EDS results of the reaction residue.

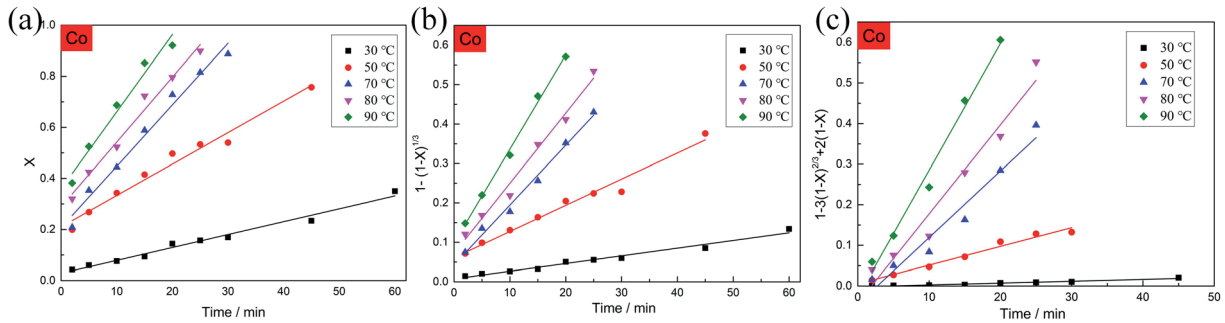

Fig. 10 Kinetics analysis of leaching Co with the leaching time at various temperatures.

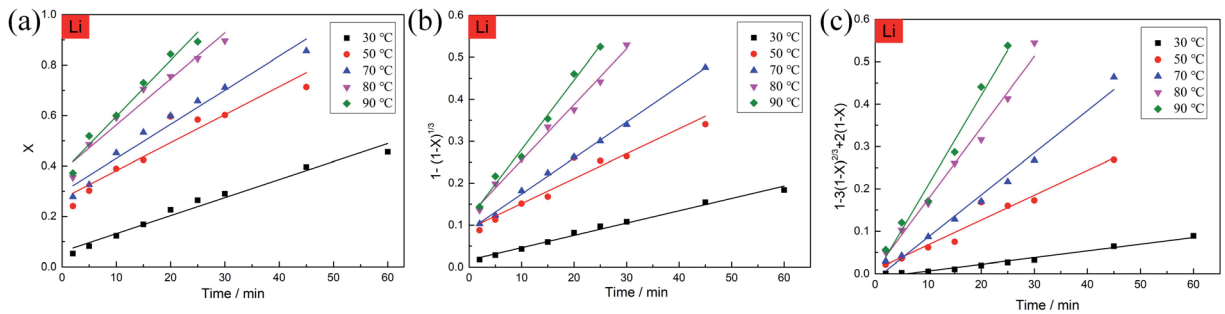

Fig. 11 Kinetics analysis of leaching Li with the leaching time at various temperatures.

According to eqn (13), the SCM equation of the three rate determination steps can be written as follows:[42]

(1) Fluid layer diffusion control:

$$X = k_1 \times t \tag{14}$$

(2) Diffusion from the solid–liquid interface control:

$$1 - (1 - X)^{\frac{1}{3}} = k_2 \times t \tag{15}$$

(3) Reaction layer control:

$$1 - 3(1 - X)^{\frac{2}{3}} + 2(1 - X) = k_3 \times t \tag{16}$$

where k_1, k_2, and k_3 are the slopes of the fitted lines, and t is the leaching time (min). Here, eqn (14), (15), and (16) are used as the mathematical model equations of the leaching process to carry out the kinetic analysis for the leaching reaction. Considering that the temperature has a significant effect on the leaching efficiency, the mathematical model was used to analyze the effect of temperature on the leaching process.

Table 2 Comparison of the R^2 values in the different kinetics model equations for Co and Li at various leaching temperatures

Elements	R^2	30 °C	50 °C	70 °C	80 °C	90 °C
Co	R_1^2	0.97998	0.97198	0.97891	0.97903	0.96231
	R_2^2	0.98127	0.98316	0.98814	0.98142	0.99451
	R_3^2	0.95001	0.97086	0.94732	0.95262	0.98296
Li	R_1^2	0.97405	0.88714	0.96028	0.95321	0.96376
	R_2^2	0.98805	0.98271	0.99745	0.99122	0.98858
	R_3^2	0.97553	0.94317	0.98070	0.98489	0.97696

For the selection of the three different models, the kinetics analysis of leaching Co with the leaching time at various temperatures are shown in Fig. 10. It is obvious that the diffusion from the solid–liquid interface control model (eqn (15)) exhibited the best fitting relevance among the other kinetics models. The same mathematical models were used to analyze the kinetics of leaching Li with the leaching time at various temperatures (Fig. 11). The fitting results of Li showed the same trend as for the leaching of Co. By comparing the R^2 values in the different kinetics model equations for Co and Li at various leaching temperatures (Table 2), the diffusion from the solid–liquid interface control model showed good correlation between the empirical kinetics equation and the experimental data.

Under optimal leaching conditions (same acid concentration, S/L ratio, and reducing agent content), the reaction rate constant of the leaching process can be described by the empirical Arrhenius law:[43]

$$\ln k = \ln A - \frac{E_a}{RT} \tag{17}$$

where A (min^{-1}) is the pre factor; E_a (J mol^{-1}) is the apparent activation energy; R (8.314 J mol^{-1} K^{-1}) is the general gas constant, and $T(k)$ is the absolute temperature. According to eqn (17), the linear relationship between $\ln k$ and $1/T$ can be described as shown in Fig. 12. Ea can be obtained from the slope of the Arrhenius fitting curve of leaching Co and Li. Table 3 shows the values for the slope and activation energies (E_a) of the leaching reactions for Li and Co. The slope values of Arrhenius fitting curve for Co and Li were −4567.66 and −3105.79, respectively. By calculation, the E_a of the leaching

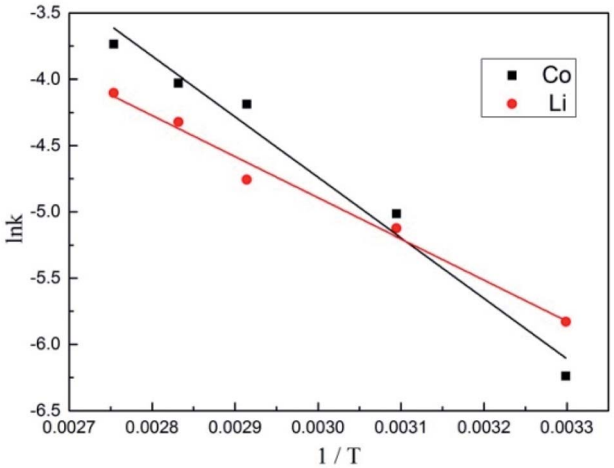

Fig. 12 Arrhenius plots for leaching Li and Co.

Table 3 Activation energies E_a for the leaching reactions for Li and Co

Elements	R^2	Slope	E_a/(kJ mol^{-1})
Co	0.98068	−4567.66	37.96
Li	0.98293	−3105.79	25.82

reactions for Co and Li were 37.96 kJ mol^{-1} and 25.82 kJ mol^{-1}. It can be seen from the table that the apparent activation energy of Co was greater than that of Li. The greater the activation energy of a substance, the higher the energy barrier that the reaction needs to overcome, and the more difficult it is to proceed. Therefore, Co was more difficult to be leached than Li. This was mainly related to the physical and chemical properties of the material. The valence state of Co in the cathode material was Co(III), and the leached Co needs to be reduced to soluble Co(II), so it needs a higher activation energy. There was no change in the valence state of Li during the reaction, so the activation energy was lower.

4 Conclusions

A mixed organic acid of citric acid and salicylic acid was used for leaching Co and Li ions from spent LIBs. In this research, a process to improve the leaching efficiencies of Co and Li was developed. Citric acid and salicylic acid were the main acids in the leaching liquid system. The results from the TG/DSC analysis showed that the optimum calcination temperature was 500 °C for 1 h and 600 °C for 3 h. The XRD and micromorphology analysis results showed that cathode material powders without impurities were obtained after pretreatment. The experimental results demonstrated that the optimal leaching efficiencies of the metals ions were 99.5% Co and 97% Li and the optimal corresponding conditions were 1.5 M citric acid, 0.2 M salicylic acid, 15 g L^{-1} S : L ratio, 6 vol% H_2O_2, 90 °C, and 90 min. Afterward, infrared tests and SEM morphology analysis indicated that only salicylic acid was present in the reaction residue after filtration because of the microsolubility of salicylic acid. Finally, it was obvious that temperature had a great influence on the leaching process though the kinetics and thermodynamic analyses. The kinetics results explained why diffusion from the solid–liquid interface control model showed good correlation with the leaching efficiencies of Co and Li. From the above results of the model, E_a values for Co and Li were obtained as 37.96 kJ mol^{-1} and 25.82 kJ mol^{-1} as provided by the suitable model of $1-(1-X)^{\frac{1}{3}} = Ae^{-\frac{E_a}{RT}} \times t$.

Author contributions

Meiling Xu: writing – original draft and writing – review & editing, Shumei Kang: conceptualization, resources, funding acquisition and supervision, Feng Jiang: conceptualization, Xinyong Yan: data curation, Zhongbo Zhu: formal analysis, Qingping Zhao: investigation, Yingxue Teng: project administration, Yu Wang: validation.

Nomenclature

LIBs	Lithium-ion batteries
LCO	Lithium cobalt oxide battery
PVC	Polyvinyl chloride
PVDF	Polyvinylidene fluoride
2θ	Diffraction angle
TG/DSC	Thermogravimetric and differential scanning calorimetry analysis
Q	Calories
M	Acid concentration index constant
S/L	Solid to liquid ratio (g L^{-1})
X	The fraction reacted (*i.e.*, leaching rate)
k_1	The slope of the fitted lines for the liquid boundary layer mass-transfer control model
k_2	The slope of the fitted lines for the surface chemical reaction control model
k_3	The slope of the fitted lines for the residue layer diffusion control model
k	The reaction rate constant in the leaching process

Conflicts of interest

The authors declared that they have no conflicts of interest with this work.

Acknowledgements

Authors are thankful to the supported by National Natural Science Foundation of China (52074149), Liaoning Provincial Department of Education support (2020LNZD07) and Joint Project of National Natural Fund of China (U1860112).

References

1 M. Idrees, L. Liu, S. Batool, H. Luo and J. Kong, Cobalt-Doping Enhancing Electrochemical Performance of Silicon/

Carbon Nanocomposite as Highly Efficient Anode Materials in Lithium-Ion Batteries, *Eng. Sci.*, 2019, **6**, 64–76.
2 X. Weilin, Z. Yajie and H. Hanbin, Cascade Extraction of Lithium in Anode of Waste Lithium Ion Battery, *Chin. J. Rare Met.*, 2020, **44**, 1078–1084.
3 X. Zhang, Y. Xie, X. Lin, H. Li and H. Cao, An overview on the processes and technologies for recycling cathodic active materials from spent lithium-ion batteries, *J. Mater. Cycles Waste Manage.*, 2013, **15**, 420–430.
4 X. Zeng, J. Li and B. Shen, Novel approach to recover cobalt and lithium from spent lithium-ion battery using oxalic acid, *J. Hazard. Mater.*, 2015, **295**, 112–118.
5 R. Sattar, S. Ilyas, H. N. Bhatti and A. Ghaffar, Resource recovery of critically-rare metals by hydrometallurgical recycling of spent lithium ion batteries, *Sep. Purif. Technol.*, 2019, **209**, 725–733.
6 Y. Li, X. Wang, Z. Wang and L. Chen, Facile Synthesis of SnO Nanorods for Na-Ion Batteries, *ES Energy Environ.*, 2019, **3**, 55–59.
7 M. Wang, Q. Tan, L. Liu and J. Li, A low-toxicity and high-efficiency deep eutectic solvent for the separation of aluminum foil and cathode materials from spent lithium-ion batteries, *J. Hazard. Mater.*, 2019, **380**, 120846.1–120846.8.
8 H. Wang, K. Huang, Y. Zhang, X. Chen, W. Jin, S. Zheng, Y. Zhang and P. Li, Recovery of lithium, nickel, and cobalt from spent lithium-ion battery powders by selective ammonia leaching and an adsorption separation system, *ACS Sustainable Chem. Eng.*, 2017, **5**, 11489–11495.
9 Z. P. Cano, D. Banham, S. Ye, A. Hintennach, J. Lu, M. Fowler and Z. Chen, Batteries and fuel cells for emerging electric vehicle markets, *Nat. Energy.*, 2018, **3**, 279–289.
10 X. Zhang, L. Li, E. Fan, Q. Xue, Y. Bian, F. Wu and R. Chen, Toward sustainable and systematic recycling of spent rechargeable batteries, *Chem. Soc. Rev.*, 2018, **47**, 7239–7302.
11 X. Zhao, P. Yang, L. Yang, Y. Cheng and Z. Guo, Enhanced Electrochemical Performance of Cu^{2+} doped TiO_2 Nanoparticles for Lithium-ion Battery, *ES Mater. Manuf.*, 2018, **1**, 67–71.
12 E. Fan, L. Li, X. Zhang, Y. Bian, Q. Xue, J. Wu, F. Wu and R. Chen, Selective Recovery of Li and Fe from Spent Lithium-Ion Batteries by an Environmentally Friendly Mechanochemical Approach, *ACS Sustainable Chem. Eng.*, 2018, **6**, 11029–11035.
13 Q. Tan and J. Li, Recycling metals from wastes: a novel application of mechanochemistry, *Environ. Technol.*, 2015, **49**, 5849–5861.
14 X. Chen, Y. Chen, T. Zhou, D. Liu, H. Hu and S. Fan, Hydrometallurgical recovery of metal values from sulfuric acid leaching liquor of spent lithium-ion batteries, *J. Waste Manage.*, 2015, **38**, 349–356.
15 L. Yan, H. Wang, H. Di and H. Luo, Electrodes with High Conductivities for High Performance Lithium/Sodium Ion Batteries, *Eng. Sci.*, 2018, **1**, 4–20.
16 C. Peng, F. P. Liu, Z. L. Wang, B. P. Wilson and M. Lundstrom, Selective extraction of lithium (Li) and preparation of battery grade lithium carbonate (Li_2CO_3) from spent Li-ion batteries in nitrate system, *Power Sources*, 2019, **415**, 179–188.
17 H. Li, E. Oraby and J. Eksteen, Extraction of copper and the co-leaching behaviour of other metals from waste printed circuit boards using alkaline glycine solutions, *Resour., Conserv. Recycl.*, 2020, **154**, 104624.
18 H. Guo, G. Kuang, H. Wan, Y. Yang, H. Z. Yu and H. D. Wang, Enhanced acid treatment to extract lithium from lepidolite with a fluorine-based chemical method, *Hydrometallurgy*, 2019, **183**, 9–19.
19 Y. Lv, L. Zhu, H. Xu, L. Yang, Z. Liu, D. Cheng, X. Cao, J. Yun and D. Cao, Core/Shell Template-Derived Co, N-Doped Carbon Bifunctional Electrocatalysts for Rechargeable Zn–Air Battery, *Eng. Sci.*, 2019, **7**, 26–37.
20 H. Tong, Q. Zhou, B. Zhang, X. Wang and W. Yu, A Novel Core–shell Structured Nickel-rich Layered Cathode Material for High-energy Lithium-ion Batteries, *Eng. Sci.*, 2019, **8**, 25–32.
21 G. Jie, H. Xiao, X. Lou, Y. Guo and Z. Guo, Enhanced Hydrometallurgical Recovery of Valuable Metals from Spent Lithium-ion Batteries by Mechanical Activation Process, *ES Energy Environ.*, 2018, **1**, 80–88.
22 P. Meshram, A. Mishra, Abhilash and R. Sahu, Environmental impact of spent lithium ion batteries and green recycling perspectives by organic acids – a review, *Chemosphere*, 2020, **242**, 125291.
23 B. Swain, J. Jeong, J. Lee, G. H. Lee and J. S. Sohn, Hydrometallurgical process for recovery of cobalt from waste cathodic active material generated during manufacturing of lithium ion batteries, *Power Sources*, 2007, **167**, 536–544.
24 J. Zhaoa, X. Qua, J. K. Qua, B. Zhanga, Z. Ninga, H. W. Xiea, X. Zhoua, Q. Songa, P. Xinga and H. Yin, Extraction of Co and Li_2CO_3 from cathode materials of spent lithium-ion batteries through a combined acid-leaching and electro-deoxidation approach, *J. Hazard. Mater.*, 2019, **379**, 120817.1–120817.7.
25 L. Sun and K. Qiu, Vacuum pyrolysis and hydrometallurgical rocess for the recovery of valuable metals from spent lithium-ion batteries, *J. Hazard. Mater.*, 2011, **194**, 378–384.
26 P. Meshram, B. Pandey and T. Mankhand, Hydrometallurgical processing of spent lithium ion batteries (LIBs) in the presence of a reducing agent with emphasis on kinetics of leaching, *Chem. Eng. J.*, 2015, **281**, 418–427.
27 M. Chena, R. Wangb, Y. Qib, Y. Hanb, R. Wangb, J. Fub, F. Mengb, X. Yib, J. Huangb and J. Shub, Cobalt and lithium leaching from waste lithium ion batteries by glycine, *Power Sources*, 2021, **482**, 228942.
28 X. Chen, C. Luo, J. Zhang, J. Kong and T. Zhou, Sustainable Recovery of Metals from Spent Lithium-Ion Batteries: A Green Process, *ACS Sustainable Chem. Eng.*, 2015, **3**, 3104–3113.
29 G. P. Nayaka, J. Manjanna, K. V. Pai, R. Vadavi, S. J. Keny and V. S. Tripathi, Recovery of valuable metal ions from the spent lithium-ion battery using aqueous mixture of mild organic

acids as alternative to mineral acids, *Hydrometallurgy*, 2015, **151**, 73–77.

30 M. Esmaeilia, S. O. Rastegara, R. Beigzadeha and T. Gub, Ultrasound-assisted leaching of spent lithium ion batteries by natural organic acids and H_2O_2, *Chemosphere*, 2020, **254**, 126670.

31 L. He, S. Y. Sun, Y. Y. Mu, X. F. Song and J. G. Yu, Recovery of lithium, nickel, cobalt, and manganese from spent lithium-ion batteries using L-tartaric acid as a leachant, *ACS Sustainable Chem. Eng.*, 2017, **5**, 714–772.

32 L. Li, W. Qu, X. Zhang, J. Lu, R. Chen, F. Wu and K. Amine, Succinic acid-based leaching system: a sustainable process for recovery of valuable metals from spent Li-ion batteries, *Power Sources*, 2015, **282**, 544–551.

33 G. L. Gao. *Leaching and recovery of spent cathode materials for lithium ion batteries by organic acid reducing system*. Shanghai University. 2019.

34 Y. P. Fu, Y. Q. He, H. C. Chen, C. L. Ye, Q. C. Lu, R. Li, W. Xie and J. Wang, Effective leaching and extraction of valuable metals from electrode material of spent lithium-ion batteries using mixed organic acids leachant, *J. Ind. Eng. Chem.*, 2019, **79**, 154–162.

35 M. B. J. G. Freitas and E. M. Garcia, Electrochemical recycling of cobalt from cathodes of spent lithium-ion batteries, *Power Sources*, 2007, **171**, 953–959.

36 Q. Meng. *Recovery and mechanism of cobalt from waste lithium cobaltite materials*. Kunming University of Science and Technology. 2018.

37 L. Lia, J. Gea, F. Wua, R. Chena, S. Chena and B. Wua, Recovery of cobalt and lithium from spent lithium ion batteries using organic citric acid as leachant, *J. Hazard. Mater.*, 2010, **176**, 288–293.

38 B. Swain, J. Jeong, J. C. Lee, G. H. Lee and J. S. Sohn, Hydrometallurgical process for recovery of cobalt from waste cathodic active material generated during manufacturing of lithium ion batteries, *Power Sources*, 2007, **167**, 536–544.

39 L. Sun and K. Qiu, Organic oxalate as leachant and precipitant for the recovery of valuable metals from spent lithium-ion batteries, *J. Waste Manage.*, 2012, **32**, 1575–1582.

40 D. A. Ferreira, L. M. Z. Prados, D. Majuste and M. B. Mansur, Hydrometallurgical separation of aluminium, cobalt, copper and lithium from spent Li-ion batteries, *Power Sources*, 2009, **187**, 238–246.

41 X. Zheng, W. Gao, X. Zhang, M. He, X. Lin, H. Cao, Y. Zhang and Z. Sun, Spent lithium-ion battery recycling – Reductive ammonia leaching of metals from cathode scrap by sodium sulphite, *J. Waste Manage.*, 2017, **60**, 680–688.

42 W. F. Gao, J. L. Song, H. B. Cao, X. Lin, X. H. Zhang, X. H. Zheng, Y. Zhang and Z. Sun, Selective recovery of valuable metals from spent lithium-ion batteries – process development and kinetics evaluation, *J. Cleaner Prod.*, 2018, **178**, 833–845.

43 W. Gao, J. Song, H. Cao, X. Lin, X. Zhang, X. Zheng, Y. Zhang and Z. Sun, Selective recovery of valuable metals from spent lithium-ion batteries – process development and kinetics evaluation, *J. Cleaner Prod.*, 2018, **178**, 833–845.